Biochemical Pharmacology 79 (2010) 239–250

Contents lists available at ScienceDirect

Biochemical Pharmacology

journal homepage: www.elsevier.com/locate/biochempharm

Mitochondria and calcium flux as targets of neuroprotection caused by minocycline in cerebellar granule cells

Eva Maria Garcia-Martinez [a,b], Sara Sanz-Blasco [c], Andonis Karachitos [d], Manuel J. Bandez [e], Francisco J. Fernandez-Gomez [a], Sergio Perez-Alvarez [a], Raquel Maria Melero Fernandez de Mera [a], Maria J. Jordan [f], Norberto Aguirre [g], Maria F. Galindo [h], Carlos Villalobos [c], Ana Navarro [e], Hanna Kmita [d], Joaquín Jordán [a,i,*]

[a] Neurofarmacología, Dpto Ciencias Médicas, Facultad de Medicina, UCLM, Albacete, Spain
[b] Servicio de Farmacia Hospitalaria, Complejo Hospitalario Universitario de Albacete, Albacete, Spain
[c] Instituto de Biología y Genética Molecular (IBGM), University Valladolid-CSIC, Valladolid, Spain
[d] Laboratory of Bioenergetics, Institute of Molecular Biology and Biotechnology, Faculty of Biology, Adam Mickiewicz University, 61-614 Poznan, Umultowska 89, Poland
[e] Bioquímica y Biología Molecular, Facultad de Medicina, University Cádiz, Cádiz, Spain
[f] Instituto Murciano de Investigación y Desarrollo Agrario y Alimentario, La Alberca, Murcia, Spain
[g] Farmacología, Facultad de Medicina, University of Navarra, Pamplona, Spain
[h] Unidad Pfizer-Castilla-La Mancha de Neuropsicofarmacología Translacional, Complejo Hospitalario Universitario de Albacete, Albacete, Spain
[i] Centro Regional de Investigaciones Biomédicas, Universidad de Castilla-La Mancha (UCLM), Albacete, Spain

ARTICLE INFO

Article history:
Received 4 June 2009
Accepted 29 July 2009

Keywords:
Anti-oxidant
Apoptosis
Voltage-dependent anion channel
Uncoupler
Aequorin
Bioluminescence

ABSTRACT

Minocycline, an antibiotic of the tetracycline family, has attracted considerable interest for its theoretical therapeutic applications in neurodegenerative diseases. However, the mechanism of action underlying its effect remains elusive. Here we have studied the effect of minocycline under excitotoxic conditions. Fluorescence and bioluminescence imaging studies in rat cerebellar granular neuron cultures using fura2/AM and mitochondria-targeted aequorin revealed that minocycline, at concentrations higher than those shown to block inflammation and inflammation-induced neuronal death, inhibited NMDA-induced cytosolic and mitochondrial rises in Ca^{2+} concentrations in a reversible manner. Moreover, minocycline added in the course of NMDA stimulation decreased Ca^{2+} intracellular levels, but not when induced by depolarization with a high K^+ medium. We also found that minocycline, at the same concentrations, partially depolarized mitochondria by about 5–30 mV, prevented mitochondrial Ca^{2+} uptake under conditions of environmental stress, and abrogated NMDA-induced reactive oxygen species (ROS) formation. Consistently, minocycline also abrogates the rise in ROS induced by 75 μM Ca^{2+} in isolated brain mitochondria. In search for the mechanism of mitochondrial depolarization, we found that minocycline markedly inhibited state 3 respiration of rat brain mitochondria, although distinctly increased oxygen uptake in state 4. Minocycline inhibited NADH–cytochrome *c* reductase and cytochrome *c* oxidase activities, whereas the activity of succinate–cytochrome *c* reductase was not modified, suggesting selective inhibition of complexes I and IV. Finally, minocycline affected activity of voltage-dependent anion channel (VDAC) as determined in the reconstituted system. Taken together, our results indicate that mitochondria are a critical factor in minocycline-mediated neuroprotection.

Abbreviations: DPPH•, 2,2-diphenyl-1-picrylhydrazyl; TPTZ, 2,4,6-tripyridyl-*S*-triazine; CM-H_2DCFDA, 5-(and 6-)-chloromethyl-2,7-dichlorodihydrofluorescein diacetate; ANT, adenine nucleotide translocase; ALS, amyotrophic lateral sclerosis; FCCP, carbonylcyanide-4-(trifluoromethoxy)-phenylhydrazone; FRAP, ferric reducing ability of plasma; $[Ca^{2+}]_{cyt}$, cytosolic Ca^{2+} concentrations; DFCA, fluorescein diacetate; GFP, green fluorescence protein; Het, hydroethidine; $[Ca^{2+}]_m$, mitochondrial Ca^{2+} concentrations; $\Delta\Psi m$, mitochondrial inner membrane potential; MPTP, mitochondrial permeability transition pore; NMDA, *N*-methyl-D-aspartic acid; ROI, region of interest; ROS, reactive oxygen species; $^{\bullet}O_2^-$, superoxide anion radical; TMRM, tetramethylrhodamine methyl ester; VDAC, voltage-dependent anion channel.

* Corresponding author at: Grupo de Neurofarmacología, Departamento de Ciencias Médicas, Universidad Castilla-La Mancha-Centro Regional de Investigaciones Biomédicas, Avda Almansa 14, Albacete 02006, Spain. Tel.: +34 967 599200; fax: +34 967599327.
E-mail address: joaquin.jordan@uclm.es (J. Jordán).

0006-2952/$ – see front matter © 2009 Elsevier Inc. All rights reserved.
doi:10.1016/j.bcp.2009.07.028

1. Introduction

Minocycline, a semi-synthetic derivate of tetracycline, is under scientific debate as a potential therapeutic agent in neurological disease processes (for review see [1,2]). Support for this new application of a time-tested antibiotic comes from observations that minocycline readily crosses the blood–brain barrier to the greatest extent of all of the tetracyclines and is well tolerated. It affords neuroprotection in experimental models of Parkinson's disease, Huntington's disease, multiple sclerosis, amyotrophic lateral sclerosis (ALS), and acute inflammation after brain trauma or cerebral ischemia [1,3]. Although there are inconsistent reports that show detrimental effects in different models of neurodegeneration [4,5], numerous studies have focused on the mechanisms underlying minocycline-mediated cell protection. However, the possible mechanisms described so far are poorly understood and need to be clarified.

We and others have postulated that mitochondria could be the pharmacological target affected by minocycline to afford cytoprotection. Proton-translocation by components of the respiratory chain generates the mitochondrial inner membrane potential ($\Delta\Psi$m). This transmembrane potential can be used to phosphorylate ADP to ATP or for Ca^{2+} uptake into mitochondria [6]. When added to isolated mitochondria, minocycline is able to decrease the $\Delta\Psi$m, possibly preventing mitochondrial permeability transition pore (MPTP) opening and the subsequent release of cytochrome *c*. Furthermore, $\Delta\Psi$m is considered an important factor in the maintenance of mitochondrial homeostasis: both Ca^{2+} uptake [7] and production of reactive oxygen species (ROS) are attenuated due to a decrease in $\Delta\Psi$m [8]. Thus, small changes in $\Delta\Psi$m may contribute to the cytoprotection mechanisms. Mitochondrial depolarization, caused by low concentrations of mitochondrial uncouplers, has been shown to be protective against NMDA-induced neuronal death [9].

Mounting evidence indicates that ROS-mediated stress plays a major role in the pathogenesis of many neurodegenerative disorders. Accordingly, it has been shown that excitotoxicity, which plays a critical role in several neurological pathologies, promotes significant increases in cytosolic Ca^{2+} concentrations ($[Ca^{2+}]_{cyt}$), ROS production, oxidative damage, and ultimately cell death [10,11]. In addition, mitochondrial Ca^{2+} overload plays a pivotal role in many cell death models including excitotoxicity [11]. Specifically, it has been reported that glutamate-induced neurotoxicity depends on mitochondrial Ca^{2+} uptake ($[Ca^{2+}]_m$) [9,12]. Under stress conditions, there is an early increase in $[Ca^{2+}]_m$ that may contribute to mitochondrial dysfunction [13,14] and MPTP opening, a point-of-no-return step in the intrinsic pathway of apoptotic cell death [15,16].

Nowadays, the molecular composition of the MPTP is still under debate. Numerous independent studies suggest that the MPTP consists of a voltage-dependent anion channel (VDAC) within the outer membrane, and adenine nucleotide translocase (ANT) within the inner membrane. The mechanism of VDAC contribution to MPTP still remains elusive. The available data indicate that pro-apoptotic stimuli can trigger a state of high or low conductance of VDAC. It has also been suggested that anti-apoptotic activity may involve an inhibitory VDAC interaction with MPTP constituents which appears critical for mitochondrial metabolite transport, volume regulation, and apoptosis (for review see [17–19]). On the other hand, there is also evidence indicating that VDAC participates in signal generation without direct involvement in subsequent processes (e.g. [20]).

Herein, we have designed several experiments to understand the mechanisms responsible for minocycline-mediated neuroprotection under excitotoxic conditions. After NMDA receptor activation, we analyzed minocycline's effect on two of the earliest events which can tip the scales in favour of neurodegeneration. Close attention was paid to the entry of Ca^{2+} through the plasma membrane, mitochondrial Ca^{2+} uptake, and generation of ROS. We also studied different parameters describing mitochondrial functions. Our results suggest that minocycline, although at concentrations higher than those shown to block inflammation and inflammation-induced neuronal death [21], prevents NMDA-induced excitotoxicity by diminishing NMDA-induced Ca^{2+} entry and altering the $\Delta\Psi$m and mitochondrial Ca^{2+} uptake. The latter may be caused by activity changes in VDAC as well as in the respiratory chain.

2. Materials and methods

2.1. Chemicals

Fura2, hydroethidine, CM-H_2DCFDA, TMRM and celenterazin were obtained from Invitrogen (Barcelona, Spain). Mitochondrial AEQ construct was a gift from Prof. Brulet (Paris, France). Culture media, sera and antibiotics are from Lonza. If not indicated otherwise, all other chemicals were purchased from Sigma or Merck.

2.2. Animals

For cerebellar granule cell cultures, 5–7-day-old Wistar rats were used. Brain mitochondria were isolated from 3-month-old male Wistar rats. All animals were housed at 22 ± 2 °C with 12 h/12 h light/dark cycles and with full access to water and food. Animal experiments were carried out in accordance with the Guiding Principles for Research Involving Animals and Human Beings of the American Physiological Society, the Guidelines of the European Union Council (86/609/CEE), and the Spanish regulations (BOE 67/8509-12, 1988) for the use of laboratory animals. Approval was obtained from the Scientific Committee of the Universities of Cádiz, Castilla-La Mancha, and Valladolid.

2.3. Cell cultures

Cerebellar granule cells were obtained as reported previously [22], plated on poly-L-lysine coated, 12 mm diameter glass coverslips. They were cultured in high-glucose, low K^+, Dulbecco's modified Eagle's medium (DMEM, Gibco, Spain) plus 10% fetal bovine serum, 5% horse serum, 100 μg/ml penicillin, and 100 μg/ml streptomycin for 2 days. Then the culture medium was replaced by Sato's medium plus 5% horse serum (to avoid excessive proliferation of glia) and cultured for 2–4 days before experiments.

2.4. Cell viability studies

To study NMDA-induced toxicity, neuronal cultures maintained 7 days *in vitro* were incubated for 30 min with 100 μM NMDA, 2 μM Ca^{2+}/Na^+ and 10 μM glycine in saline solution. Treatments were terminated by washing cells three times with Krebs solution before incubating with regular medium. Minocycline was added 10 min before NMDA at different concentrations and maintained during the whole experiment. Cell viability was analyzed 24 h later using the fluorescein diacetate/propidium iodide double-staining procedure. Living and dead cells were counted in 3–4 coverslips per condition (a total of 300–450 cells per coverslip) and normalized to corresponding controls. At least three independent experiments were used for quantification.

2.5. Fluorescence imaging of cytosolic $[Ca^{2+}]$

Coverslips containing cerebellar granule cells were incubated in standard medium containing (in mM) NaCl 145, KCl 5, $CaCl_2$ 1,

$MgCl_2$ 1, glucose 10, Hepes 10 (pH 7.42), and loaded with 4 μM fura2/AM for 60 min at room temperature. Coverslips were then placed on the heated stage of an inverted Zeiss microscope (Axiovert S100 TV), and while continuously perfused with the same pre-warmed standard medium, epi-illuminated alternately at 340 and 380 nm. Light emitted above 520 nm was recorded with an OrcaER Hamamatsu camera (Hamamtsu Photonics, Hamamatsu, Japan). Pixel-by-pixel ratios of consecutive frames were captured, and $[Ca^{2+}]_{cyt}$ was estimated from these ratios as previously reported [23].

2.6. Bioluminescence imaging of mitochondrial $[Ca^{2+}]$

Cerebellar granule cells were transfected with plasmids containing GFP-aequorin targeted to mitochondria [24] using a Nucleofector II® device and the VPG-1003 transfection kit (Amaxa Biosystems, Cologne, Germany). After 24 h, cells were incubated for 1 h with 1 μM coelenterazine, washed, and placed into a perfusion chamber set at 37 °C under a Zeiss Axiovert S100 TV microscope. They were then perfused at 5–10 ml/min with test solutions based on the standard perfusion solution pre-warmed to 37 °C as described above. At the end of each experiment, cells were permeabilized with 0.1 mM digitonin in 10 mM $CaCl_2$ in order to release all the residual aequorin counts. Bioluminescence images were taken with a Hamamatsu VIM photon counting camera handled with an Argus-20 image processor. Photonic emissions were integrated for 10 s periods. Photons/cell in each image was quantified using the Hamamatsu Aquacosmos software. Total counts per region of interest (ROI) ranged between 2×10^3 and 2×10^5, and noise was (mean ± SD) 1 ± 1 counts per second (c.p.s.) per typical cell area (2000 pixels). Data were first quantified as rates of photoluminescence emission/total c.p.s. remaining at each time (% of remaining counts) and divided by the integration period (L/L_{TOTAL} in s^{-1}). Emission values of less than 4 c.p.s. were not used for calculations. Calibrations in terms of $[Ca^{2+}]_{mit}$ were performed as previously reported [23]. Briefly, the total luminescence for every ROI was computed by adding up the values of all images. In addition, the following values were registered for every time point (t): L = luminescence emission at time t; sum (L) = ΣL values from $t = 0$ to t; L_{TOTAL} (L_{T1}) = total luminescence remaining at time t = total (L) − sum (L); % remaining luminescence = $100 \times L_{TOTAL}$/total (L); and ratio (R) = L/L_{T1}. Finally, $[Ca^{2+}]$ was calculated using the following algorithm:

$$[Ca^{2+}]\,(\text{in M}) = [R + (R \times K_{TR}) + 1]/[(K_R - (R \times K_R)],$$

where $R = L/L_{T1} \times \lambda)]^{(1/n)}$, using the constant values K_R, K_{TR}, n and λ reported previously (see [23] for a detailed description). In some experiments, cells were permeabilized with 20 μM digitonin in "intracellular" medium with the following composition: 130 mM KCl, 10 mM NaCl, 1 mM $MgCl_2$, 1 mM K_3PO_4, 0.2 mM EGTA, 1 mM ATP, 20 μM ADP, 2 mM succinate, 20 mM Hepes/KOH, pH 6.8. Cells were then incubated for 5 min with the same medium containing 200 nM Ca^{2+} (buffered with EGTA), with or without minocycline. Finally, perfusion was switched to "intracellular" medium containing 5 μM Ca^{2+}, with or without minocycline.

2.7. Mitochondrial potential

The effects of treatment on $\Delta\Psi$ in intact cerebellar granule cells were estimated by fluorescence imaging of cells loaded with the $\Delta\Psi$ sensitive probe tetramethylrhodamine methyl ester (TMRM), one the most sensitive probes available [25]. Briefly, cerebellar granule cells were loaded with 10 nM TMRM for 10 min, washed with a standard, external medium, and placed on the perfusion chamber of a Zeiss Axiovert S100 TV inverted microscope. Cells were then continuously perfused with pre-warmed (37 °C) external medium, with and without treatments. Fluorescence images were taken at 10 s intervals with a Hamamatsu VIM photon counting camera handled with an Argus-20 image processor. Traces from individual cells were normalized relative to the value before the addition of either vehicle or treatment and averaged. Background fluorescence after collapse of the mitochondrial potential induced by 10 μM FCCP was subtracted. Further details have been reported previously [26].

2.8. Superoxide intracellular production

Superoxide production was monitored using hydroethidine (HEt, Molecular Probes) as described previously [27]. Coverslips containing cerebellar granule cells were incubated in standard medium containing (in mM): NaCl 145, KCl 5, $CaCl_2$ 1, $MgCl_2$ 1, glucose 10, and Hepes 10 (pH 7.42) and loaded with 10 μM hydroethidine. Next, coverslips were placed on the heated stage of an inverted Nikon (Eclipse TE2000) microscope. Light emitted above 535 nm was recorded with an emission filter of 635 nm (Omega Optical) with an OrcaER Hamamatsu camera (Hamamatsu Photonics, Hamamatsu, Japan). Background was subtracted. Frames were recorded every 10 s over a 7 min period. Linear regression of fluorescence data was obtained of each condition and the slope of the best fitting line was taken as an index of superoxide anion radical ($^{\bullet}O_2^-$) production.

2.9. Isolation of mitochondria and preparation of mitochondrial membranes

Brain mitochondria were isolated from the whole rat brain in a small Potter homogenizer with a Teflon pestle. Homogenization was carried out in a medium of 230 mM mannitol, 70 mM sucrose, 1.0 mM EDTA, and 10 mM Tris–HCl, pH 7.40, at a ratio of 9 ml of homogenization medium/g of tissue. The homogenate was centrifuged at $700 \times g$ for 10 min and the supernatant at $8000 \times g$ for 10 min to precipitate mitochondria that were washed in the same conditions [28]. The obtained mitochondrial suspensions of about 20 mg protein/ml were used immediately after isolation for the determination of respiration or frozen in liquid N_2 and kept at −80 °C. Sub-mitochondrial membranes (disrupted mitochondria) were obtained from brain mitochondria that were twice frozen-and-thawed and homogenized each time by passage through a tuberculin needle. The procedure yielded a preparation of disrupted mitochondria with 0.20–0.24 nmol cytochrome aa_3/mg protein, subsequently used for the determination of enzymatic activity of the respiratory complexes and the presence of markers of oxidative damage. The protein content of the samples was determined using Folin reagent and bovine serum albumin as the standard. To study the effects of minocycline, the brain-coupled mitochondria or sub-mitochondrial membranes were added or incubated for 5 min at 4 °C, respectively, with 0, 75, 100, 125, or 150 μM minocycline.

2.10. Mitochondrial oxygen uptake

The oxygen uptake of rat brain mitochondria (0.7–0.8 mg/ml) was determined with a Clark electrode in a 1.5 ml chamber at 30 °C, in an air-saturated reaction medium consisting of: 0.23 M mannitol, 0.07 M sucrose, 20 mM Tris–HCl, 1 mM EDTA, 5 mM phosphate, 4 mM $MgCl_2$, at pH 7.4. Respiration rates were determined with 5 mM malate–5 mM glutamate or 6 mM succinate as substrates, and state 3 respiration was established by addition of 0.5 mM ADP. Mitochondria oxygen uptake was assayed in uncoupled mitochondria with 1 μM FCCP. Three determinations were performed for each value.

2.11. Measurement of ROS levels in mitochondrial suspension

Mitochondrial ROS production was evaluated with the fluorescent probe 5-(and 6-)-chloromethyl-2,7-dichlorodihydrofluorescein diacetate (CM-H_2DCFDA) in isolated mitochondrial suspension. CM-H_2DCFDA is a reduced form of fluorescein diacetate (DFCA) that requires oxidation before becoming fluorescent. Therefore, any measurable change in fluorescence intensity can be directly related to changes in free radical activity, mainly the generation of hydrogen peroxide and hydroxyl radicals. Mitochondrial suspensions were incubated with CM-H_2DCFDA (10 μg/ml), and fluorescence intensity was measured in a Spectra Max Gemini XS (Molecular Devices, Sunnyvale, CA). Brain mitochondria were challenged with 75 μM Ca^{2+} to induce ROS formation during 30 min with or without minocycline. Experiments were performed in 96-multiwell plates including four samples for each experimental point. The average of relative DFCA fluorescence from at least three separate mitochondrial preparations was determined. Results are expressed as mean ± SEM values.

2.12. Mitochondrial electron transfer activity

The enzymatic activity of complexes I–III, II–III, and IV were determined spectrophotometrically at 30 °C with sub-mitochondrial membranes suspended in 60 mM phosphate buffer (pH 7.4) with corresponding substrates added. For NADH–cytochrome *c* reductase (the activity of complexes I and III) and succinate–cytochrome *c* reductase (the activity of complexes II and III), mitochondrial membranes were added with 0.20 mM NADH or 5.0 mM succinate as substrates, 0.10 mM cytochrome c^{3+}, and 1.0 mM KCN. The enzymatic activity determined at 550 nm ($\varepsilon = 19\ mM^{-1}\ cm^{-1}$), with the results expressed as nmol cytochrome *c* reduced/min × mg protein. Cytochrome oxidase (complex IV) was determined in the same buffer with 0.05 mM cytochrome c^{2+} added, prepared by reduction with ascorbate, and filtration across a Sephadex G25 column. The rate of cytochrome *c* oxidation was calculated as the first order reaction constant (k') per mg protein, and expressed as nmol cytochrome *c* oxidized at 10 μM cytochrome *c*/min × mg protein. This result determines the electron transfer rates of physiological respiration [29]. Three determinations for each value.

2.13. DPPH radical-scavenging activity

The scavenging activity of minocycline was measured according to the method described by Brand-Williams et al. [30] with some modifications. Briefly, 500 μl of minocycline methanolic solutions (100 μM) at different concentrations (12.5–150 μl/ml) were added to 1 ml of 2,2-diphenyl-1-picrylhydrazyl (DPPH•) methanolic solution (0.1 mM). Estimated time of reaction (20 min) was determined considering the reduction of absorbance at 517 nm (monitored every 5 min) until the reaction curve reached a plateau. The absorbance was measured at room temperature, in darkness, with a blank (500 μl of sample plus 1 ml of methanol). The absorbance of the control (500 μl of methanol in 1 ml of DPPH• solution) was measured daily. All of the assays were conducted in triplicate. The percentage activity for the DPPH• technique was calculated according to % discoloration = [1 − (Abs sample/Abs control)] × 100.

2.14. Ferric reducing ability assay

The ferric reducing ability of minocycline was measured according to the method developed by Benzie and Strain [31]. Anti-oxidant compounds are able to reduce ferric compounds to ferrous-TPTZ, which develops a blue color with a maximum absorption at 593 nm. FRAP reagent was freshly prepared from 300 mM acetate buffer (pH 3.6), 10 mM 2,4,6-tripyridyl-*S*-triazine (TPTZ) made up in 40 mM HCl, and 20 mM $FeCl_3 \cdot 6H_2O$ solution. All three solutions were mixed together in the ratio of 10:1:1 (v/v/v). An aliquot of 40 μl of minocycline was added to 1.2 ml of FRAP reagent. The absorption of the reaction mixture was measured at 593 nm after 2 min of incubation at 37 °C. Measurements were performed in triplicate. Fresh working solutions of known Fe (II) concentrations ($FeSO_4 \cdot 7H_2O$, 0–2 mM) were used for calibration. The anti-oxidant capacity, based upon the ability to reduce ferric ions of each sample, was calculated from the linear calibration curve and expressed as mmol $FeSO_4$ equivalents.

2.15. Isolation of VDAC from Saccharomyces cerevisiae mitochondria

The yeast *Saccharomyces cerevisiae* M3 cells (MATα, lys2, his4, trp1, ade2, leu2, ura3) [32] were grown at 28 °C in YPG medium (1% yeast extract, 2% peptone, 3% glycerol) at pH 5.5 to OD_{546} of 2.2. Mitochondria and the mitochondrial outer membrane were isolated according to the published procedure [33]. The obtained outer membrane pellet was suspended in the solubilization buffer containing 3% Triton X-100, 10 mM Tris–HCl (pH 7.0) and 1 mM EGTA, and was incubated for 30 min at 0 °C. The suspension was then loaded onto a dry hydroxyapatite/celite column [34] and the first two fractions were collected. Before reconstitution, the preparations of VDAC were checked by Western blotting with anti-yeast anti-serum for the presence of marker proteins of mitochondrial compartments as well as for VDAC (not shown).

2.16. Conductance measurements in planar phospholipid membranes

Membranes were formed from soybean asolectin suspended at concentration of 25 mg/ml in *n*-decane, across a circular hole (aperture diameter about 250 μm) in the thin wall of a Delrin chamber (Warner Instruments) separating two compartments (*cis*–*trans*) filled with unbuffered 1 M KCl, pH 7.0. The chamber was connected to the recording equipment through a matched pair of Ag–AgCl electrodes. Preparations of VDAC were added in small aliquots (2–3 μl) to the *cis* compartment. *Cis* also refers to the compartment where the voltage was held. Signals were amplified by a BLM-120 bilayer amplifier (Bio-LOGIC Science Instruments) and computer software was used for data collection. The average amount of analyzed insertion events for a given set of conditions was 70.

2.17. Statistics

When only two means were compared, Student's *t*-test was used. For more than two groups, statistical significance of the data was assessed by analysis of the variance (ANOVA) and compared using Tukey's test. Differences were considered significant at $p < 0.05$. For the conductance measurements in planar phospholipid membranes, the differences between calculated values of average conductance were tested by *t*-test (at $\alpha = 0.01$) for statistical significance.

3. Results

3.1. Minocycline and cell viability

Consistent with previous data from our laboratory and elsewhere, minocycline afforded cytoprotection to neuronal cultures when exposed to excitotoxic conditions. Cerebellar granular cells were treated with minocycline at different concentrations (1–150 μM) and challenged with NMDA (100 μM) during 30 min. Twenty-four hours later, neuronal viability was evaluated by using

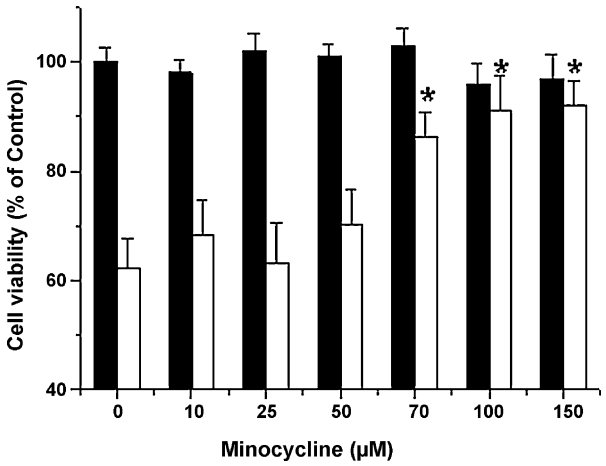

Fig. 1. Minocycline protects neuronal cultures against excitotoxic stimulus in a concentration-dependent manner. After 7 days *in vitro*, cultured cerebellar granule cells were exposed to 100 μM NMDA for 30 min. Minocycline (10–150 μM) was added 10 min before exposure to NMDA and maintained until the end of experiment. Cell viability was assayed 24 h later. Black bars in this figure represent treatment with the indicated minocycline concentrations in the absence of NMDA. The data represent mean ± SD of at least nine coverslips (three independent cell cultures). $^{*}p < 0.01$ different from 0 minocycline and NMDA (analysis of the variance and Tukey's test).

fluorescein diacetate and the propidium iodide staining method. As shown in Fig. 1, NMDA treatment decreased cell viability by about 35% ($p < 0.05$). Pre-treatment with minocycline, which did not affect cell viability (Fig. 1, black bars), afforded neuroprotection in a concentration-dependent manner. Concentrations lower than 50 μM did not significantly modify NMDA-induced cell death (Fig. 1).

3.2. Minocycline and calcium signals

It has been clearly established that NMDA-induced cell death depends on Ca^{2+} entry through the plasma membrane and mitochondrial Ca^{2+} uptake [12]. We therefore studied the effects of minocycline on NMDA-induced increases in cytosolic ($[Ca^{2+}]_{cyt}$) and mitochondrial Ca^{2+} ($[Ca^{2+}]_{mit}$) concentrations in cerebellar granule cells. Fig. 2A shows pseudocolor images of a representative microscopic field corresponding to $[Ca^{2+}]_{cyt}$ levels during perfusion with the glutamate receptor agonist NMDA (100 μM) in the presence of minocycline (100 μM) and after its removal. We found that in the presence of 100 μM minocycline, NMDA-induced a rather modest increase in $[Ca^{2+}]_{cyt.}$ Five min after minocycline withdrawal, cells were stimulated again with NMDA and $[Ca^{2+}]_{cyt}$ was monitored. Under these experimental conditions, NMDA increased $[Ca^{2+}]_{cyt}$ to a much larger extent ($p < 0.001$, $n = 4$) indicating that minocycline inhibits Ca^{2+} entry to cells mediated by activation of NMDA receptor channel (Fig. 2A). This result is consistent with our previous findings that minocycline decreases the amplitude and the number of excitatory postsynaptic currents with EC_{50} between 42 and 64 μM, indicating that glutamatergic synaptic transmission is drastically affected by neuroprotective concentrations of minocycline (30 μM or higher [35]).

To study the effects of minocycline on $[Ca^{2+}]_{mit}$ cerebellar granule cells were transfected with mitochondria-targeted aequorin, a bioluminescent probe widely used for subcellular Ca^{2+} measurements [22,23]. This probe also contains GFP to help selecting transfected cells for bioluminescence imaging. Cerebellar granule cells were transfected with the GA plasmid and incubated for 24 h to allow for the expression of the Ca^{2+} probe. Fig. 2B shows the bioluminescence (AEQ) and fluorescence (GFP) images of transfected cerebellar granule cells. We found that NMDA, in the

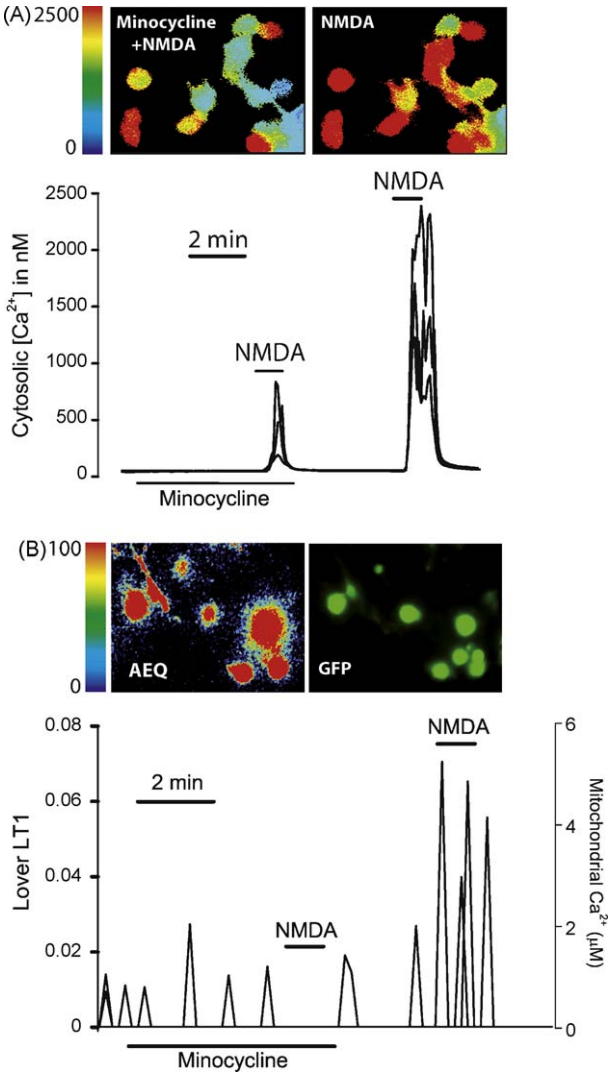

Fig. 2. Minocycline inhibits the increases in cytosolic and mitochondrial $[Ca^{2+}]$ induced by NMDA. (A) Cerebellar granule cells were loaded with fura2/AM and $[Ca^{2+}]_{cyt}$ levels were monitored by fluorescence microscopy. Pictures show $[Ca^{2+}]_{cyt}$ levels (coded in pseudocolor, color scale 0–2500 nM) during perfusion with NMDA (100 μM) with and without minocycline (100 μM). Traces show recordings of $[Ca^{2+}]_{cyt}$ in individual, representative cerebellar granule cells. ($n = 193$ cells, four independent experiments). (B) Cerebellar granule cells were transfected with GA plasmid. 24 h later were incubated with coelenterazine for 2 h at room temperature and subjected to $[Ca^{2+}]_{mit}$ measurements by photon counting imaging. Pictures show the bioluminescence (AEQ) and fluorescence (GFP) images of transfected cells. Color scale 0–100 photonic emissions per pixel. Traces show recordings of $[Ca^{2+}]_{mit}$ in individual, representative cerebellar granule cells ($n = 11$ cells, two independent experiments).

presence of 100 μM minocycline, failed to induce any rise in $[Ca^{2+}]_{mit}$. However, after removal of minocycline, NMDA promoted the increase in $[Ca^{2+}]_{mit}$ ($n = 2$). Thus, these results indicate that minocycline inhibits both the cytosolic and the mitochondrial rises in Ca^{2+} concentrations induced by NMDA in a reversible manner.

To address whether minocycline inhibits the increase in $[Ca^{2+}]_{cyt}$ in a specific manner, we studied the effects of minocycline on $[Ca^{2+}]_{cyt}$ induced by either NMDA or high K^+ medium, added here to promote opening of voltage-gated Ca^{2+} channels. Fig. 3 shows that minocycline blocked NMDA-induced $[Ca^{2+}]_{cyt}$ rise but failed to reduce the increased $[Ca^{2+}]_{cyt}$ induced by a high K^+ medium. Traces are mean ± SEM values of all cells present in representative experiments. These data indicate that minocycline does not inhibit voltage-gated Ca^{2+} channels that can be activated by NMDA-induced plasma membrane depolarization.

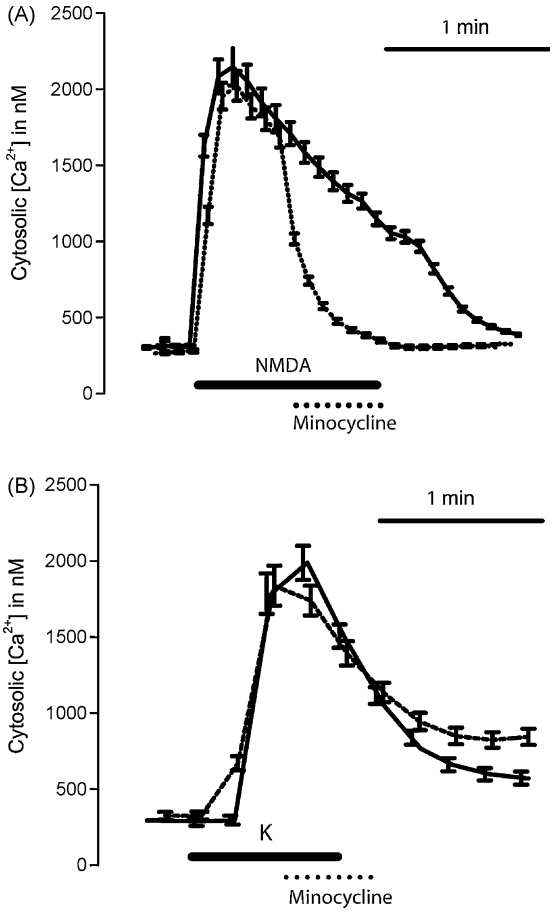

Fig. 3. Minocycline decreases cytosolic Ca^{2+} levels when added in the presence of NMDA but not in the presence of high K^+ medium. Cerebellar granule cells were loaded with fura2/AM and $[Ca^{2+}]_{cyt}$ levels were monitored by fluorescence microscopy. Traces show the effect of minocycline (100 μM) over the increased $[Ca^{2+}]_{cyt}$ induced by NMDA (100 μM) (A) or high K^+ (B) medium. Traces are mean ± SEM values of $[Ca^{2+}]_{cyt}$ on all cells present in the same microscopic field and are representative of at least three independent experiments.

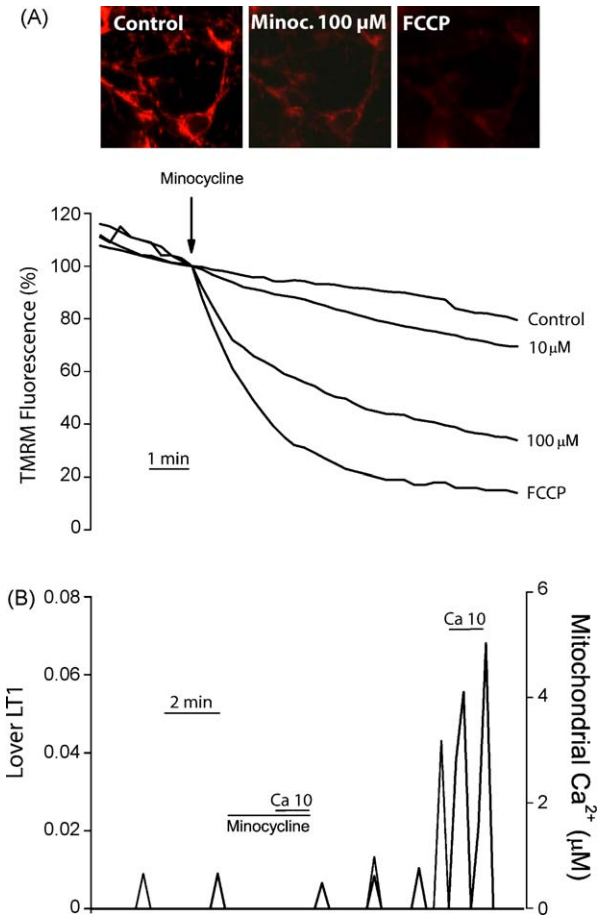

Fig. 4. Minocycline depolarizes mitochondria and inhibits mitochondrial Ca^{2+} uptake. (A) Cerebellar granule cells were loaded with 10 nM TMRM for monitoring the effects of minocycline on the mitochondrial inner membrane potential. Pictures show TMRM staining of the same cells before and after treatment with 10 and 100 μM minocycline and 10 μM FCCP. Traces show average recordings of TMRM fluorescence in representative experiments. Fluorescence values were normalized to the value before treatment and averaged (n = 50 cells, three experiments). (B) Cerebellar granule cells were transfected with GA plasmid, cultured for 24 h and incubated with coelenterazine for 2 h at room temperature. Cells were permeabilized by digitonin in intracellular medium (see Section 2) and subjected to bioluminescence imaging of mitochondrial $[Ca^{2+}]$. Permeabilized cells were stimulated with intracellular medium containing 10 μM $[Ca^{2+}]$ in the presence of 100 μM minocycline and after its removal. Traces shown are recordings from representative, individual cells (n = 36 cells, six independent experiments).

In the next set of experiments we studied whether minocycline may affect the mitochondrial inner membrane potential and mitochondrial Ca^{2+} uptake acting on intact cells. Cerebellar granule cells were loaded with the mitochondrial inner membrane potential probe TMRM and subjected to fluorescence microscopy. Fig. 4A shows TMRM staining of cerebellar granule cells before and after the addition of 100 μM minocycline. An image of the same cells after adding the mitochondrial uncoupler FCCP is also shown. Perfusion of TMRM-loaded cells with minocycline induced a dose-dependent decrease in TMRM fluorescence consistent with a mitochondrial depolarization. This effect was absent at 1 μM minocycline (not shown), slightly apparent at 10 μM and quite strong at 100 μM. As expected, the mitochondria uncoupler FCCP (10 μM) caused organelle depolarization (Fig. 4A). Therefore, these results indicate that minocycline depolarizes mitochondria in intact cells in a dose-dependent manner. Minocycline decreases TMRM fluorescence at 10 and 100 μM by 17 ± 4% and 70 ± 6%, respectively, relative to the effect of the total uncoupler FCCP at 10 μM. We have shown previously that decreases in TMRM fluorescence can be used to estimate mitochondrial potential decrements [26]. According to the algorithm proposed [26], we estimate that minocycline, at 10–100 μM, depolarizes mitochondria in intact cerebellar granule cells by 5–30 mV.

We have reported recently that a weak depolarization of mitochondria may largely influence mitochondrial Ca^{2+} uptake [26]. Accordingly, we studied whether minocycline inhibited mitochondrial Ca^{2+} uptake in permeabilized cells exposed to Ca^{2+} concentrations similar to those achieved in Ca^{2+} microdomains (10 μM). Cerebellar granule cells were transfected with the GA plasmid and incubated for 24 h. Then cells were incubated with digitonin and subjected to bioluminescence imaging. Fig. 4B shows that addition of Ca^{2+} to permeabilized cells in the presence of 100 μM minocycline failed to rise $[Ca^{2+}]_{mit}$. After removal of minocycline, addition of Ca^{2+} induced release of photonic emissions corresponding to a increase in $[Ca^{2+}]_{mit}$ (n = 36 cells, six independent experiments). Therefore, these results indicate that minocycline induces mitochondrial depolarization to such an extent that inhibits mitochondrial Ca^{2+} uptake.

3.3. Minocycline and ROS production

Increasing amount of data indicates that ROS play a major role in the pathogenesis of neurodegenerative disorders [16] and also in excitotoxic cell death models [36]. As shown in Fig. 5A, cerebellar granular neurons challenged with NMDA (100 μM) showed a higher rate of oxidation of dihydroethidine, an indicator of

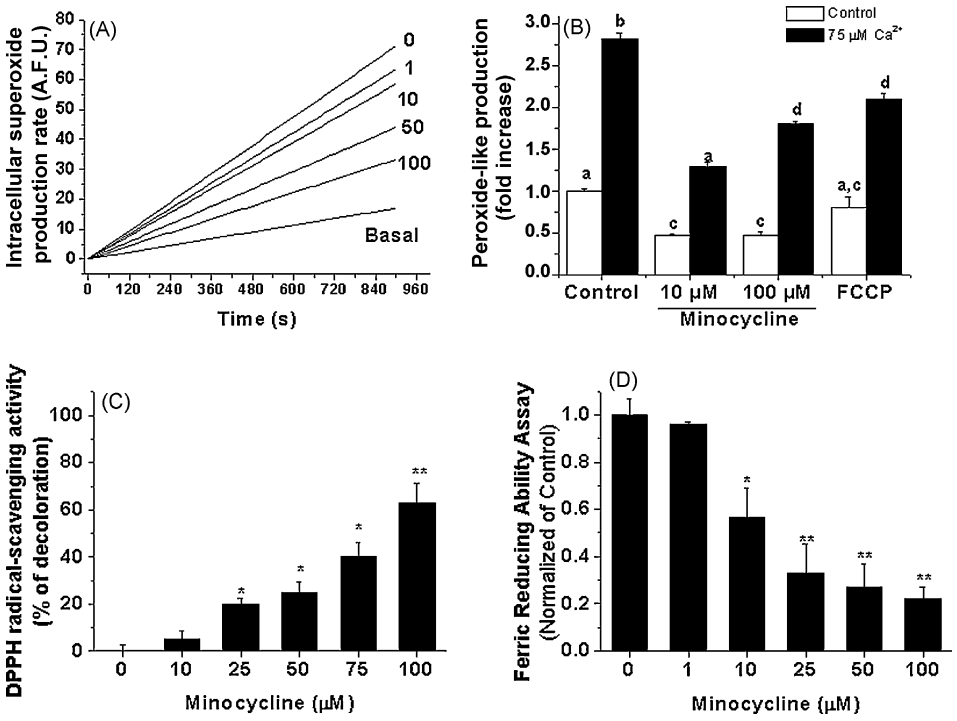

Fig. 5. Minocycline presents anti-oxidant functions. (A) Minocycline declines intracellular superoxide production rate induced by NDMA (100 μM) in cerebellar granular cells. The slopes of the lines fitting the fluorescence intensity changes (an index of the rate of superoxide production) were individually measured and averaged. At least 84 individual cells were averaged to calculate the slope. The mean slope values were used to generate a theoretical line using the following equation: $y = ax$. The figure represents generated lines of O_2^- production in both basal conditions and during 100 μM NMDA with and without minocycline (1, 10, 50 and 100 μM). (B) Minocycline abrogates ROS production caused by 75 μM Ca^{2+} in brain isolated mitochondria. DFCA fluorescence was measured 30 min after the addition of Ca^{2+} to mitochondrial suspensions. Data are mean ± SD, of at least four different preparations. Columns marked with the same small letters denotes values not significantly different ($p > 0.05$). (C and D) Minocycline showed a DPPH radical scavenger activity (C) and mediates the reduction of Fe^{3+} to Fe^{2+} (FRAP) (D). The data represent mean ± SD of at least four or three independent experiments. $^*p < 0.05$, $^{**}p < 0.001$ vs. control conditions (without minocycline).

superoxide anion production. Specifically, cerebellar granular neurons presented a basal superoxide production rate of 0.019 ± 0.0023 A.F.U./min ($n = 78$). The addition of NMDA (100 μM) induced an increase in the rate of superoxide production, to a value of 4.18 ± 0.9645 A.F.U./min ($n = 186$). The effect that was abrogated by minocycline in a concentration-dependent manner.

In order to ascertain whether minocycline blocked ROS production at the mitochondrial level, we used CM-H_2DCFDA to measure peroxide-like formation in brain isolated mitochondria challenged with high Ca^{2+}. First, minocycline decreased basal mitochondrial ROS production (Fig. 5B). The addition of 75 μM Ca^{2+} to the mitochondrial suspension resulted in a significant increase in the production of ROS (2.8-fold increase). Minocycline inhibited this increase (Fig. 5B). In addition, the mitochondrial uncoupler FCCP (10 μM) was also able to inhibit the increase in ROS production induced by the applied concentration of Ca^{2+} (Fig. 5B).

Taking into account these results, we went further to explore whether minocycline might function as a superoxide dismutase (SOD) or a catalase mimetic in a cell free system. Our results revealed that minocycline does not show any of the above mentioned enzymatic activities (data not shown). Interestingly, and consistent with previous data, minocycline showed a diphenylpicrylhydrazyl (DPPH) radical scavenger activity [37], an effect that reached statistical significance at a concentration of 25 μM and above (Fig. 5C). Furthermore, our data also confirmed that minocycline-mediated the reduction of Fe^{3+} to Fe^{2+}, at concentrations higher than 10 μM (Fig. 5D).

3.4. Minocycline-induced effects on mitochondrial function

The O_2 uptake of isolated rat brain mitochondria was determined in resting state, in phosphorylating state and in uncoupled state triggered by FCCP. Malate–glutamate and succinate were used as respiratory substrates in the presence of minocycline in the range of 75–125 μM. Figs. 6 and 7 present typical recordings of the oxygen uptake obtained in the presence of 125 μM minocycline for phosphorylating state (Fig. 6) and resting and uncoupled states (Fig. 7). Minocycline increased the oxygen uptake in resting state, by

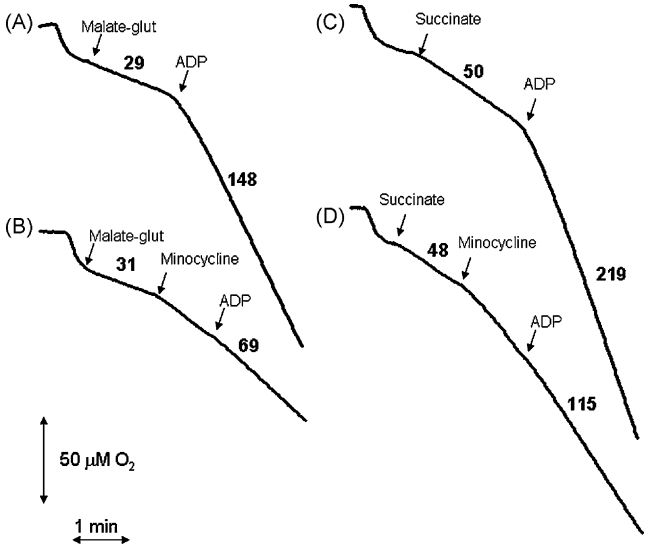

Fig. 6. Mitochondrial oxygen uptake of rat brain mitochondria in phosphorylating state. Respiratory rates were determined at 30 °C. Additions: mitochondria (0.7–0.8 mg/ml), 5 mM malate–5 mM glutamate, 6 mM succinate, 0.5 mM ADP and 125 μM minocycline. The numbers near the traces indicates oxygen uptake in ng-at O/min × mg protein.

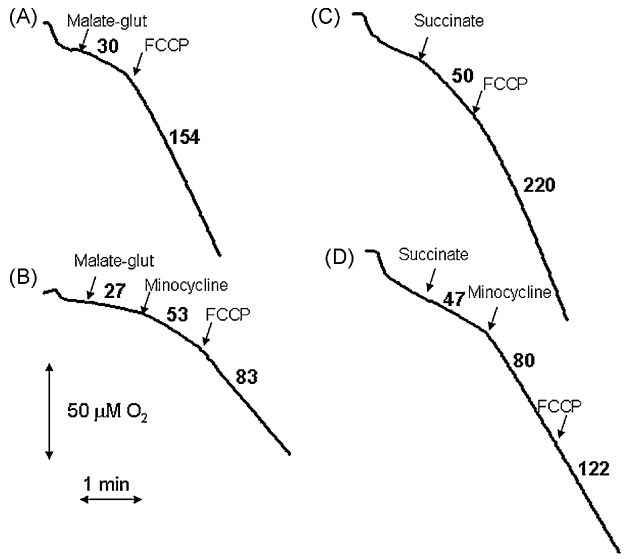

Fig. 7. Mitochondrial oxygen uptake of rat brain mitochondria in resting state and in uncoupled state induced by FCCP. Respiratory rates were determined at 30 °C. Additions: mitochondria (0.7–0.8 mg/ml) 5 mM malate–5 mM glutamate, 6 mM succinate, 0.1 μM FCCP and 125 μM minocycline. The numbers near the traces indicates oxygen uptake in ng-at O/min × mg protein ($n = 3$).

about 80% in the case of malate–glutamate as respiratory substrate and by about 60% with succinate as respiratory substrate but simultaneously decreased the uncoupling capacity of FCCP by about 50% for the both respiratory substrates. However, in phosphorylating state minocycline caused decrease in oxygen uptake, by about 60% in the case of malate–glutamate as respiratory substrate and by about 50% with succinate as respiratory substrate. The effect of minocycline on the oxygen uptake by brain mitochondria in uncoupled state in the presence of malate–glutamate and succinate as respiratory substrates were similar to that observed for phosphorylating state and the calculated levels of inhibition were about 50% and 45%, respectively. The inhibition was not caused by minocycline-mediated rupture of the mitochondrial outer membrane as minocycline did not cause increase in cytochrome *c* release (not shown). Fig. 8 summarizes the effect of different concentrations of minocycline on the oxygen uptake during the studied respiratory states. Independently of the studied respiratory substrate we observed minocycline concentration-dependent inhibition of phosphorylating and uncoupled states and stimulation of resting state. However, the obtained calibration curves differed in shape between malate–glutamate and succinate that suggests differences of the applied mechanisms. Therefore we analyzed the influence of minocycline on enzymatic activities of the respiratory chain complexes I + III (NADH–cytochrome *c* reductase), II + III (succinate–cytochrome *c* reductase), and IV (cytochrome *c* oxidase). As shown in Fig. 9, minocycline in the range of 75–150 μM inhibited markedly complexes I + III and IV. Thus minocycline appeared to affect the oxygen uptake supported by malate–glutamate at the level of complexes I and IV and the oxygen uptake supported by succinate only at the level of complex IV.

3.5. Minocycline affects VDAC conductance and voltage dependence

There is a growing amount of data showing that the voltage-dependent anion channel is a dynamic regulator, or governor, of mitochondrial functions (for review see [17,18]). Therefore we have studied the effects of minocycline on channel-forming activity of VDAC reconstituted into lipid bilayers. It was achieved by adding VDAC preparation to the aqueous phase of one side (so called *cis* side) of a black membrane bilayer made of asolectin. It is

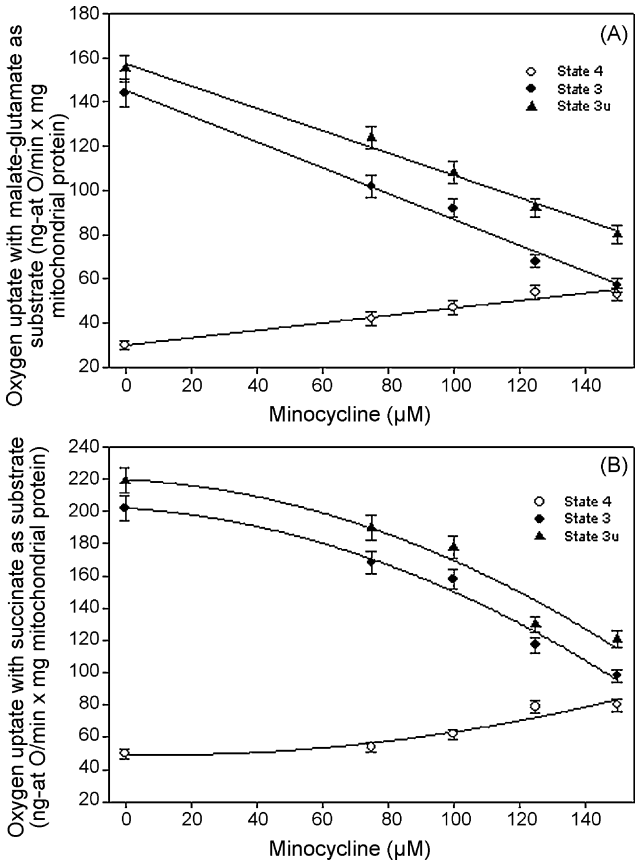

Fig. 8. Effects of minocycline on the mitochondrial oxygen uptake of rat brain mitochondria in state 4, state 3 (0.5 mM ADP) and state 3 u (0.1 μM FCCP) ($n = 3$). Respiratory rates are determined with mitochondria (0.7–0.8 mg/ml) at 30 °C. (Panel A) 5 mM malate, 5 mM glutamate as respiratory substrate; (panel B) 10 mM succinate as substrate.

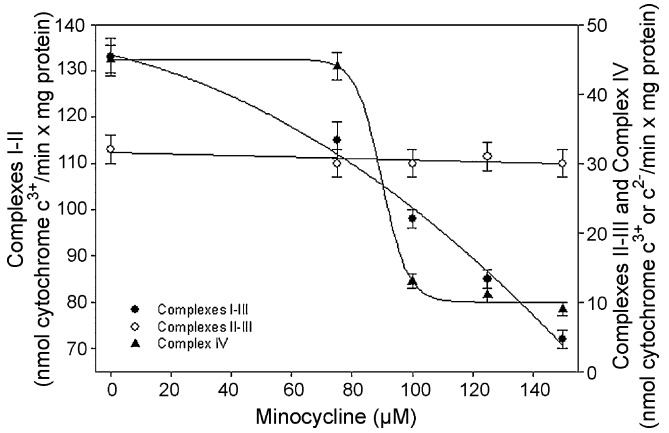

Fig. 9. Effects of minocycline on the electron transfer activities of rat brain mitochondrial membranes. NADH–cytochrome *c* reductase activity (complexes I–III) and succinate–cytochrome *c* reductase activity (complexes II + III) expressed as nmol cytochrome *c* reduced/min × mg protein; and cytochrome oxidase activity (complex IV) expressed as nmol cytochrome *c* oxidized at 10 μM cytochrome *c*/min × mg protein ($n = 3$).

well known that VDAC behavior in planar phospholipid membranes made of asolectin is voltage-dependent and symmetrical [38–40], meaning that the channel closes at about the same rate and to about the same extent depending on the applied potential value but regardless its sign. Thus, VDAC reconstituted into planar phospholipid membranes displays the ability to adopt a fully open state and multiple closed states of significantly smaller conduc-

tance that differ in permeability. The VDAC protein was isolated from mitochondria of the yeast *S. cerevisiae* that contain only one channel-forming VDAC isoform [41] and are commonly used as a model to study mitochondrial biology. Since 100 μM minocycline did not change formation and stability of the planar phospholipid membrane (not shown), we perform comparative experiments at different values of the applied positive and negative potential and in the presence of different concentrations of minocycline. The obtained distributions of conductances in 1 M KCl were used to build histograms and to calculate values of average conductance of VDAC under a given experimental conditions.

The effect imposed by minocycline on VDAC conductance did not depend on the sign of the applied potential and was clearly visible under conditions of the dominance of VDAC fully open state, i.e., at a membrane potential of 10 mV. Examples of single channel insertions at a membrane potential of +10 mV shown in Fig. 10A indicate that unexpectedly minocycline caused flickering of VDAC conductance in the second or even millisecond time scale dependently of minocycline concentration. Single channel insertions were then used to create histograms. Fig. 10B presents histograms obtained at +10 mV and in the presence of increasing concentrations of minocycline. Addition of minocycline distinctly changed distribution of VDAC conductance and consequently caused decrease in calculated values of average conductance dependently of its concentration (Fig. 10C). The calculated values of average conductance at +10 mV were as follows (in nS): 3.9 ± 0.1 nS (in the absence of minocycline), 3.4 ± 0.3 (10 μM minocycline), 3.2 ± 0.4 (50 μM minocycline) and 2.9 ± 0.4 (100 μM minocycline). This denotes a serious change in a functional state of VDAC towards lower conductance states as the dominance of VDAC closure observed at +70 mV corresponded to an average conductance of 1.9 ± 0.2 nS. The observed effect imposed by minocycline on VDAC conductance could result from changes in voltage dependence of the channel. Voltage dependence can be observed in reconstitution systems and is defined as the probability of a channel occurrence in a given conductance state depending on the value of the applied potential [32,42]. As shown in Fig. 10D, in the absence as well as in the presence of minocycline an increase in the value of the applied potential facilitated closure of the studied channels that resulted in a decrease of the value of an average conductance calculated for a given potential (G). This, in turn, caused a decrease in the value of the ratio G/G_0, where G_0 denotes an average conductance at the lowest applied potential (10 mV). The sign of the applied potential did not influence these changes. However, in the presence of minocycline the VDAC voltage dependence was less pronounced and the weakening was concentration-dependent.

4. Discussion

The present data, built upon our group's previous work [22,35,43], posits the intricate involvement of mitochondria in minocycline-mediated cytoprotection for neuronal cells. Following excitotoxic NMDA receptor activation, the accumulation of Ca^{2+} and the generation of ROS are modulated as minocycline targets mitochondria. Intervention with minocycline may prove useful as these are two events that occur early in neurodegenerative processes.

Consistent with previous observations [44,45], minocycline afforded cytoprotection to neuronal cultures under conditions of NMDA receptor-mediated excitotoxicity, although at a concentration range higher than that needed to block inflammation and inflammation-induced neuronal death [21]. In cultures pre-treated with minocycline, the NMDA-induced $[Ca^{2+}]_{cyt}$ rise was dramatically inhibited. We can exclude this effect as a consequence of the well established association between tetracyclines and Ca^{2+} buffer capacity [43]. Minocycline failed to modify the intracellular levels of Ca^{2+} in resting conditions, and did not attenuate a Ca^{2+} increase following cellular depolarization with 50 mM KCl. Our data also revealed that this effect was reversible, demonstrated when minocycline removal allowed neurons to respond to NMDA in a similar extent as control cell cultures. Furthermore, minocycline actually decreased $[Ca^{2+}]_{cyt}$ during the course of NMDA receptor stimulation. This later result might explain recent studies showing minocycline blocking centrally mediated hyperalgesia induced by intrathecal NMDA [46], or shed some light on the favourable effects of minocycline in a therapeutic window between 6 and 24 h after a stroke [47].

Minocycline does more than just preventing Ca^{2+} fluxes at the plasma membrane. It also reduced $[Ca^{2+}]_{mit}$ overload, a pivotal role in excitotoxicity and other models of cell death [9,12,15]. By using bioluminescence imaging with mitochondria-targeted aequorin, we directly observed the effects of minocycline on NMDA-induced mitochondrial Ca^{2+} overload. This effect remained in permeabilized cells as minocycline abrogated mitochondrial Ca^{2+} uptake induced by Ca^{2+} concentrations that surpass the activation of the mitochondrial Ca^{2+} uniporter. Supporting the hypothesis that small changes in mitochondrial potential may dramatically influence mitochondrial Ca^{2+} uptake, minocycline, at 100 μM, decreased by about 5–30 mV the $\Delta\Psi$m in cerebellar granular cells. Therefore, minocycline reduces the electrochemical driving force required for mitochondrial Ca^{2+} uptake, resulting in the prevention of $[Ca^{2+}]_{mit}$ overload in excitotoxicity. Accordingly, prevention of mitochondrial Ca^{2+} uptake by the mitochondrial Ca^{2+} uncoupler FCCP largely abrogated NMDA-induced cell death [9]. Therefore, minocycline inhibit mitochondrial Ca^{2+} overload induced by NMDA acting both at the plasma membrane level and at the mitochondrial level. These two actions seem independent as FCCP does not prevent NMDA-induced Ca^{2+} influx (data not shown).

Minocycline also weakened ROS production, both in cultured neurons and in isolated mitochondria. Minocycline reduced the rate of increase of hydroethidine oxidation in neurons exposed to NMDA. Minocycline also reduced peroxide-like generation in isolated mitochondria suspensions when challenged with 75 μM Ca^{2+}. Similar to minocycline's effect on $\Delta\Psi$m, this anti-oxidant action was mimicked by the mitochondrial uncoupler FCCP. We cannot exclude a structure-dependent anti-oxidant effect of minocycline, since previous findings [48] have shown a direct DPPH radical-scavenging property and the capacity to reduce Fe^{3+}. However, such properties failed to afford SOD or catalase activity of minocycline. We have previously shown that minocycline does not prevent malonate-induced peroxide formation in cerebellar granular cell [22], and is unable to prevent ROS-mediated MPTP opening that supporting the above statement [43].

Consistent with a role of mitochondria as a target of minocycline-mediated neuroprotection, we found that minocycline affects distinctly activity of the respiratory chain although the observed effect is rather complicated. First, minocycline inhibits complex I and complex IV of the respiratory chain. Interestingly, only these two complexes are true proton pumps within the respiratory chain able to physically move protons across a membrane [49]. Nevertheless, the observed inhibition occurs in phosphorylating and uncoupled states supported by malate–glutamate or by succinate. On the other hand, the inhibition limits uncoupling capacity of uncoupler (FCCP) although minocycline added during resting state stimulate the oxygen uptake that might be caused by uncoupling as minocycline is able to decrease the inner membrane potential. However, the uncoupling effect is rather weak when compared to that of FCCP. The apparent contradictory effects of minocycline on mitochondrial respiration (i.e., stimulation vs. inhibition) have been, in part, previously reported for others drugs such as local anaesthetics [50]. Since

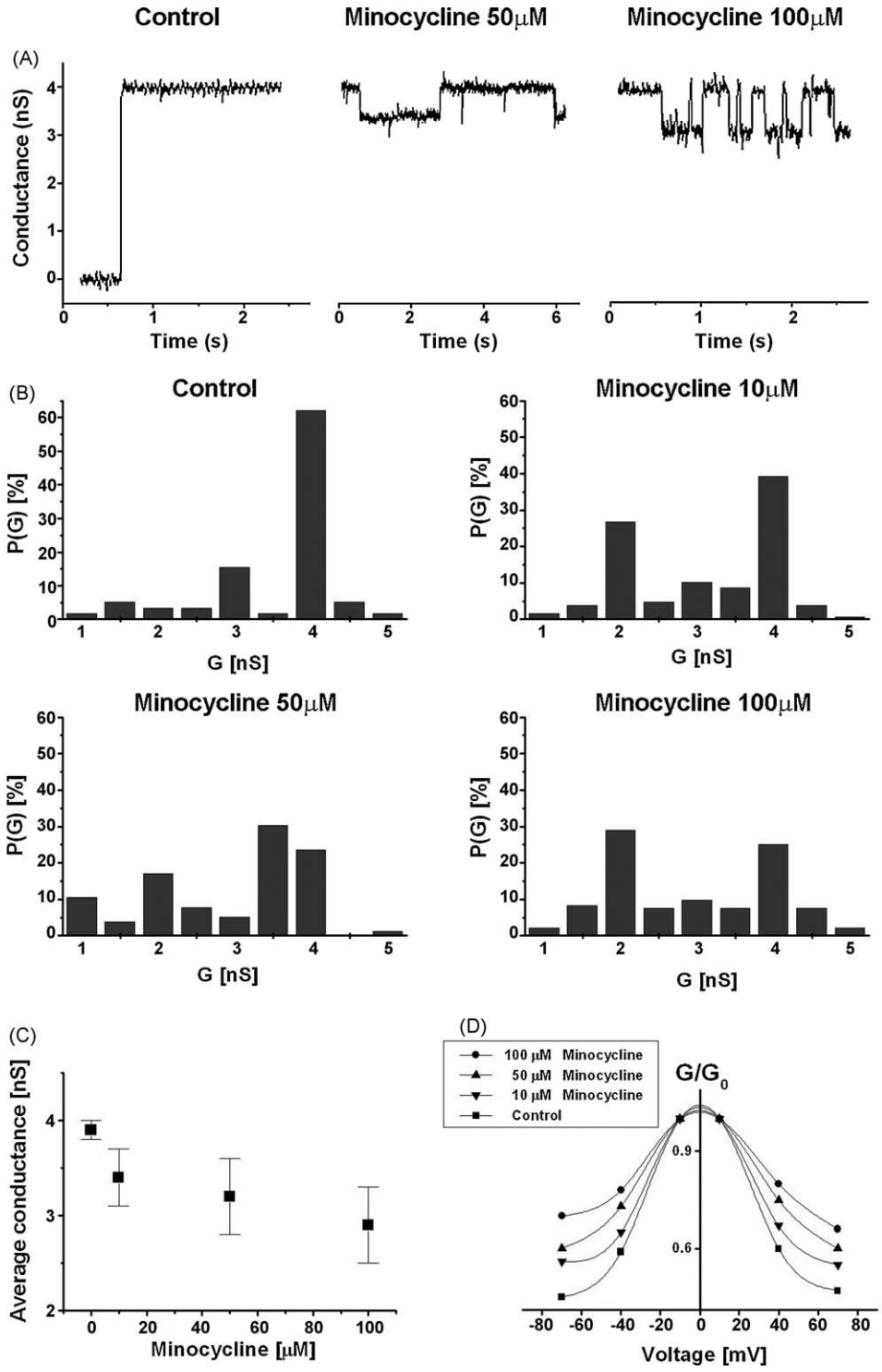

Fig. 10. The effect of minocycline on reconstituted VDAC. (A) Examples of single channel insertions in the presence of increasing minocycline concentrations at a membrane potential of +10 mV. (B) Histograms of VDAC conductances obtained in the presence of increasing minocycline concentrations at a membrane potential of +10 mV. P(*G*) is the probability that a given conductance increment *G* is observed. (C) VDAC average conductance as a function of minocycline concentration. Values of average conductance were calculated at a membrane potential of +10 mV. The dominance of VDAC closure at a membrane potential of +70 mV corresponded to an average conductance of 1.9 ± 0.2 nS. (D) The dependence of VDAC on the applied potential in the presence of minocycline increasing concentrations. G/G_0 is the ratio of the conductance (G) at a given voltage and the conductance (G_0) at the lowest applied potential (10 mV). The average amount of analyzed insertion events for a given conditions used to calculate average conductance was 70. The obtained values of average conductance were statistically different.

activation of NMDA receptors responsible for excitotoxicity imposes a high energetic demand on the *in situ* mitochondria [51] one could hypothesize that minocycline exerts its neuroprotective effect by affecting bioenergetic functions of mitochondria. Indeed, this effect could be responsible for the recent report showing that minocycline has a harmful effect on patients with ALS [52]. Accordingly, it was proposed by Kupsch et al. [53] that minocycline impairs mitochondria functions causing $\Delta\psi$ dissipation. Subsequently, deenergized mitochondria lose the ability to undergo Ca^{2+}-triggered MPTP resulting in cell death.

Minocycline might also act as a modulator of the voltage-dependent anion channel. Minocycline added to a reconstituted system caused VDAC transition into lower conductance states and decreased the voltage dependence in a concentration-dependent way. Thus, in the presence of minocycline the voltage dependence of reconstituted VDAC is weaker although simultaneously the channel is modified to assume lower conductance states that suggests an effect of minocycline on VDAC gating mechanism [39]. Furthermore flickering of VDAC conductance observed in the presence of minocycline might result from VDAC transient blockade/closure [54]. This, in turn, could have anti-apoptotic effects [19]. Moreover, VDAC closing is accompanied by a change of its selectivity toward cations (e.g. [38,40]). However, it has been recently proven that VDAC also has a cation selective open state [55]. Therefore, it was proposed by Mannella and Kinnally [18] that VDAC modulators triggering a transition to lower conductance states might not be acting to close but to open. Nevertheless in the presence of minocycline, the permeability of the mitochondrial outer membrane that is mediated by VDAC might be affected, thus contributing to neuroprotection. In support of this view is the neuroprotective activity of rasagiline, a known anti-Parkinsonian drug, related to its ability to modulate VDAC [56]. Noteworthy, minocycline does not change formation or stability of the planar phospholipid membrane as measured by reconstitution experiments. This implies the absence of nonspecific perturbations of lipid membranes by minocycline. However, it cannot be excluded that minocycline acts at the protein–lipid interface causing redistribution of membrane lateral pressure sensed by specific membrane proteins [57].

In conclusion, the results obtained support a pleiotropic mechanism of minocycline neuroprotective activity that involves direct interaction of minocycline with proteins (e.g. with VDAC), minocycline-mediated changes in the interface between lipids and membrane proteins (e.g. VDAC, NMDA receptor, complexes of the respiratory chain) and anti-oxidant effects of minocycline that control protein activity (e.g. MPTP opening). Although further investigations are required to clarify these mechanisms based in our results (Fig. 11) we can propose that minocycline affects VDAC activity, as well as the mitochondrial respiratory chain at the level of complexes I and IV and NMDA-induced entry of Ca^{2+}. As a result, minocycline may contribute to change the mitochondrial inner membrane potential, to ROS formation, and to mitochondrial Ca^{2+} uptake. The effects of minocycline on mitochondria complement its influence on NMDA-mediated Ca^{2+} influx into the cytosol, as changes in cytosolic Ca^{2+} concentration may in turn affect mitochondrial respiration, potentially leading to the prevention of NMDA-mediated excitotoxicity that is also conveyed by mitochondria; as lowering of cytosolic Ca^{2+} concentration inhibits formation and opening of MPTP crucial for apoptotic cell death. Simultaneously, formation and opening of MPTP may be inhibited by minocycline directly and/or indirectly due to its intricate effect on mitochondria. Therefore, under pathological conditions, minocycline may prove beneficial in preventing apoptotic signalling via stabilization of mitochondria-mediated signal cascades.

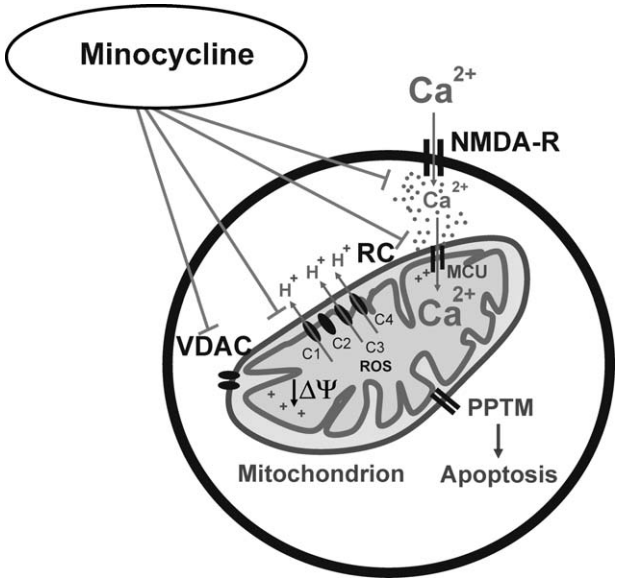

Fig. 11. A model of minocycline-mediated neuroprotection. Minocycline inhibits Ca^{2+} entry supported by NMDA receptor being a hallmark of excitotoxicity. In addition, minocycline modulates both VDAC and the respiratory chain (RC) leading to mitochondrial depolarization. Mitochondrial depolarization diminishes the driving force for mitochondrial Ca^{2+} uptake through the mitochondrial Ca^{2+} uniporter (MCU), which prevents mitochondrial Ca^{2+} overload, ROS production and apoptosis execution. These pleiotropic effects may contribute to explain the neuroprotection afforded by minocycline.

Acknowledgments

We are in debit to Ichiro Ikuta and Prof. Pedro Tranque for review and recommendations. Dr. Mercedes Lorenzo and Aymara Valdivia are thanked for their help with catalase and SOD activities experiments. We are grateful to Vanesa Guijarro and Sandra Arteaga for technical assistance and Piotr Bednarczyk for his help. This work was supported by SAF2008-05143-C03-1 from CICYT: Investigación sobre drogodependiencias. Ministerio de Sanidad y Consumo (04005-00) and PI2007/55 Consejería de Sanidad from Junta de Comunidades de Castilla-La Mancha (to J.J.) and by "CCM Obra Social y Cultural-FISCAM" and "Incorporación de grupos emergentes" FIS CARLOS III (to M.F.G.). RM M-F is a Bellow FPU. S.P-A. is a fellow from the Spanish Ministerio de Sanidad y Consumo. SAF2008-05143-C03-2 to N.A. M.J.J thanks financial support from the European Social Fund.

References

[1] Blum D, Chtarto A, Tenenbaum L, Brotchi J, Levivier M. Clinical potential of minocycline for neurodegenerative disorders. Neurobiol Dis 2004;17:359–66.
[2] Jordan J, Fernandez-Gomez FJ, Ramos M, Ikuta I, Aguirre N, Galindo MF. Minocycline and cytoprotection: shedding new light on a shadowy controversy. Curr Drug Deliv 2007;4:225–31.
[3] Kim HS, Suh YH. Minocycline and neurodegenerative diseases. Behav Brain Res 2009;196:168–79.
[4] Mievis S, Levivier M, Communi D, Vassart G, Brotchi J, Ledent C, et al. Lack of minocycline efficiency in genetic models of Huntington's disease. Neuromol Med 2007;9:47–54.
[5] Goni-Allo B, Ramos M, Jordan J, Aguirre N. In vivo studies on the protective role of minocycline against excitotoxicity caused by malonate or N-methyl-d-aspartate. Exp Neurol 2005;191:326–30.
[6] Chalmers S, Nicholls DG. The relationship between free and total calcium concentrations in the matrix of liver and brain mitochondria. J Biol Chem 2003;278:19062–70.
[7] White RJ, Reynolds IJ. Mitochondria accumulate Ca^{2+} following intense glutamate stimulation of cultured rat forebrain neurons. J Physiol 1997;498(Pt 1):31–47.
[8] Votyakova TV, Reynolds IJ. DeltaPsi(m)-dependent and -independent production of reactive oxygen species by rat brain mitochondria. J Neurochem 2001;79:266–77.
[9] Pivovarova NB, Nguyen HV, Winters CA, Brantner CA, Smith CL, Andrews SB. Excitotoxic calcium overload in a subpopulation of mitochondria triggers delayed death in hippocampal neurons. J Neurosci 2004;24:5611–22.
[10] Lafon-Cazal M, Pietri S, Culcasi M, Bockaert J. NMDA-dependent superoxide production and neurotoxicity. Nature 1993;364:535–7.
[11] Reynolds IJ, Hastings TG. Glutamate induces the production of reactive oxygen species in cultured forebrain neurons following NMDA receptor activation. J Neurosci 1995;15:3318–27.
[12] Stout AK, Raphael HM, Kanterewicz BI, Klann E, Reynolds IJ. Glutamate-induced neuron death requires mitochondrial calcium uptake. Nat Neurosci 1998;1:366–73.
[13] Kristian T, Siesjo BK. Calcium in ischemic cell death. Stroke 1998;29:705–18.
[14] Zaidan E, Sims NR. The calcium content of mitochondria from brain subregions following short-term forebrain ischemia and recirculation in the rat. J Neurochem 1994;63:1812–9.

[15] Norenberg MD, Rao KV. The mitochondrial permeability transition in neurologic disease. Neurochem Int 2007;50:983–97.
[16] Bernardi P, Scorrano L, Colonna R, Petronilli V, Di Lisa F. Mitochondria and cell death. Mechanistic aspects and methodological issues. Eur J Biochem 1999;264:687–701.
[17] Lemasters JJ, Holmuhamedov E. Voltage-dependent anion channel (VDAC) as mitochondrial governator—thinking outside the box. Biochim Biophys Acta 2006;1762:181–90.
[18] Mannella CA, Kinnally KW. Reflections on VDAC as a voltage-gated channel and a mitochondrial regulator. J Bioenerg Biomembr 2008;40:149–55.
[19] Kroemer G, Galluzzi L, Brenner C. Mitochondrial membrane permeabilization in cell death. Physiol Rev 2007;87:99–163.
[20] Rostovtseva TK, Bezrukov SM. VDAC regulation: role of cytosolic proteins and mitochondrial lipids. J Bioenerg Biomembr 2008;40:163–70.
[21] Tikka TM, Koistinaho JE. Minocycline provides neuroprotection against N-methyl-D-aspartate neurotoxicity by inhibiting microglia. J Immunol 2001; 166:7527–33.
[22] Fernandez-Gomez FJ, Gomez-Lazaro M, Pastor D, Calvo S, Aguirre N, Galindo MF, et al. Minocycline fails to protect cerebellar granular cell cultures against malonate-induced cell death. Neurobiol Dis 2005;20:384–91.
[23] Nunez L, Senovilla L, Sanz-Blasco S, Chamero P, Alonso MT, Villalobos C, et al. Bioluminescence imaging of mitochondrial Ca^{2+} dynamics in soma and neurites of individual adult mouse sympathetic neurons. J Physiol 2007;580:385–95.
[24] Rogers KL, Stinnakre J, Agulhon C, Jublot D, Shorte SL, Kremer EJ, et al. Visualization of local Ca^{2+} dynamics with genetically encoded bioluminescent reporters. Eur J Neurosci 2005;21:597–610.
[25] Voronina SG, Barrow SL, Gerasimenko OV, Petersen OH, Tepikin AV. Effects of secretagogues and bile acids on mitochondrial membrane potential of pancreatic acinar cells: comparison of different modes of evaluating DeltaPsim. J Biol Chem 2004;279:27327–38.
[26] Nunez L, Valero RA, Senovilla L, Sanz-Blasco S, Garcia-Sancho J, Villalobos C. Cell proliferation depends on mitochondrial Ca^{2+} uptake: inhibition by salicylate. J Physiol 2006;571:57–73.
[27] Bindokas VP, Jordan J, Lee CC, Miller RJ. Superoxide production in rat hippocampal neurons: selective imaging with hydroethidine. J Neurosci 1996;16: 1324–36.
[28] Navarro A, Boveris A. Rat brain and liver mitochondria develop oxidative stress and lose enzymatic activities on aging. Am J Physiol Regul Integr Comp Physiol 2004;287:R1244–9.
[29] Navarro A, Gomez C, Lopez-Cepero JM, Boveris A. Beneficial effects of moderate exercise on mice aging: survival, behavior, oxidative stress, and mitochondrial electron transfer. Am J Physiol Regul Integr Comp Physiol 2004;286: R505–11.
[30] Brand-Williams W, Cuvelier ME, Berset C. Use of free radical method to evaluate antioxidant activity. LWT-Food Sci Technol 1995;28:25–30.
[31] Benzie IF, Strain JJ. The ferric reducing ability of plasma (FRAP) as a measure of "antioxidant power": the FRAP assay. Anal Biochem 1996;239:70–6.
[32] Schein SJ, Colombini M, Finkelstein A. Reconstitution in planar lipid bilayers of a voltage-dependent anion-selective channel obtained from paramecium mitochondria. J Membr Biol 1976;30:99–120.
[33] Daum G, Gasser SM, Schatz G. Import of proteins into mitochondria. Energy-dependent, two-step processing of the intermembrane space enzyme cytochrome b2 by isolated yeast mitochondria. J Biol Chem 1982;257:13075–80.
[34] de Pinto V, Prezioso G, Palmieri F. A simple and rapid method for the purification of the mitochondrial porin from mammalian tissues. Biochim Biophys Acta 1987;905:499–502.
[35] Gonzalez JC, Egea J, Del Carmen Godino M, Fernandez-Gomez FJ, Sanchez-Prieto J, Gandia L, et al. Neuroprotectant minocycline depresses glutamatergic neurotransmission and $Ca^{(2+)}$ signalling in hippocampal neurons. Eur J Neurosci 2007;26:2481–95.
[36] Dykens JA, Stern A, Trenkner E. Mechanism of kainate toxicity to cerebellar neurons in vitro is analogous to reperfusion tissue injury. J Neurochem 1987;49:1222–8.
[37] Morimoto N, Shimazawa M, Yamashima T, Nagai H, Hara H. Minocycline inhibits oxidative stress and decreases in vitro and in vivo ischemic neuronal damage. Brain Res 2005;1044:8–15.
[38] Colombini M, Blachly-Dyson E, Forte M. VDAC, a channel in the outer mitochondrial membrane. Ion Channels 1996;4:169–202.
[39] Karachitos A, Galganska H, Wojtkowska M, Budzinska M, Stobienia O, Bartosz G, et al. Cu,Zn-superoxide dismutase is necessary for proper function of VDAC in *Saccharomyces cerevisiae* cells. FEBS Lett 2009;583:449–55.
[40] Benz R. Permeation of hydrophilic solutes through mitochondrial outer membranes: review on mitochondrial porins. Biochim Biophys Acta 1994;1197:167–96.
[41] Blachly-Dyson E, Song J, Wolfgang WJ, Colombini M, Forte M. Multicopy suppressors of phenotypes resulting from the absence of yeast VDAC encode a VDAC-like protein. Mol Cell Biol 1997;17:5727–38.
[42] Liu MY, Colombini M. A soluble mitochondrial protein increases the voltage dependence of the mitochondrial channel, VDAC. J Bioenerg Biomembr 1992;24:41–6.
[43] Fernandez-Gomez FJ, Galindo MF, Gomez-Lazaro M, Gonzalez-Garcia C, Cena V, Aguirre N, et al. Involvement of mitochondrial potential and calcium buffering capacity in minocycline cytoprotective actions. Neuroscience 2005;133:959–67.
[44] Tikka T, Fiebich BL, Goldsteins G, Keinanen R, Koistinaho J. Minocycline, a tetracycline derivative, is neuroprotective against excitotoxicity by inhibiting activation and proliferation of microglia. J Neurosci 2001;21:2580–8.
[45] Pi R, Li W, Lee NT, Chan HH, Pu Y, Chan LN, et al. Minocycline prevents glutamate-induced apoptosis of cerebellar granule neurons by differential regulation of p38 and Akt pathways. J Neurochem 2004;91:1219–30.
[46] Hua XY, Svensson CI, Matsui T, Fitzsimmons B, Yaksh TL, Webb M. Intrathecal minocycline attenuates peripheral inflammation-induced hyperalgesia by inhibiting p38 MAPK in spinal microglia. Eur J Neurosci 2005;22:2431–40.
[47] Lampl Y, Boaz M, Gilad R, Lorberboym M, Dabby R, Rapoport A, et al. Minocycline treatment in acute stroke: an open-label, evaluator-blinded study. Neurology 2007;69:1404–10.
[48] Kraus RL, Pasieczny R, Lariosa-Willingham K, Turner MS, Jiang A, Trauger JW. Antioxidant properties of minocycline: neuroprotection in an oxidative stress assay and direct radical-scavenging activity. J Neurochem 2005;94:819–27.
[49] Nicholls DG, Ferguson SJ. Bioenergetics 3. London: Academic Press; 2002.
[50] Sun X, Garlid KD. On the mechanism by which bupivacaine conducts protons across the membranes of mitochondria and liposomes. J Biol Chem 1992;267: 19147–54.
[51] Yadava N, Nicholls DG. Spare respiratory capacity rather than oxidative stress regulates glutamate excitotoxicity after partial respiratory inhibition of mitochondrial complex I with rotenone. J Neurosci 2007;27:7310–7.
[52] Gordon PH, Moore DH, Miller RG, Florence JM, Verheijde JL, Doorish C, et al. Efficacy of minocycline in patients with amyotrophic lateral sclerosis: a phase III randomised trial. Lancet Neurol 2007;6:1045–53.
[53] Kupsch K, Hertel S, Kreutzmann P, Wolf G, Wallesch CW, Siemen D, et al. Impairment of mitochondrial function by minocycline. FEBS J 2009;276:1729–38.
[54] Tan W, Loke YH, Stein CA, Miller P, Colombini M. Phosphorothioate oligonucleotides block the VDAC channel. Biophys J 2007;93:1184–91.
[55] Pavlov E, Grigoriev SM, Dejean LM, Zweihorn CL, Mannella CA, Kinnally KW. The mitochondrial channel VDAC has a cation-selective open state. Biochim Biophys Acta 2005;1710:96–102.
[56] Youdim MB, Weinstock M. Molecular basis of neuroprotective activities of rasagiline and the anti-Alzheimer drug TV3326 [(N-propargyl-(3R)aminoindan-5-YL)-ethyl methyl carbamate]. Cell Mol Neurobiol 2001;21:555–73.
[57] Cantor RS. The lateral pressure profile in membranes: a physical mechanism of general anesthesia. Biochemistry 1997;36:2339–44.